

$(m, d, N) = (1, 3, 2)$ Lifshitz point and the three-dimensional XY universality class studied by high-temperature bivariate series for XY models with anisotropic competing interactions

P. Butera^{1,*} and M. Pernici^{2,†}

¹*Istituto Nazionale di Fisica Nucleare, Sezione di Milano-Bicocca, 3 Piazza della Scienza, 20126 Milano, Italy*

²*Istituto Nazionale di Fisica Nucleare, Sezione di Milano, 16 Via Celoria, 20133 Milano, Italy*

(Received 7 May 2008; published 6 August 2008)

High-temperature bivariate expansions have been derived for the two-spin-correlation function in a variety of classical lattice XY (planar rotator) models in which spatially isotropic interactions among first-neighbor spins compete with spatially isotropic or anisotropic (in particular uniaxial) interactions among next-to-nearest-neighbor spins. The expansions, calculated for cubic lattices of dimensions $d=1, 2$, and 3 , are expressed in terms of the two variables $K_1=J_1/kT$ and $K_2=J_2/kT$, where J_1 and J_2 are the nearest-neighbor and the next-to-nearest-neighbor exchange couplings, respectively. This paper deals in particular with the properties of the $d=3$ uniaxial XY model (ANNNXY model) for which the bivariate expansions have been computed through the 18th order, thus extending by 12 orders the results so far available and making a study of this model possible over a wide range of values of the competition parameter $R=J_2/J_1$. Universality with respect to R on the critical line separating the paramagnetic and the ferromagnetic phases can be verified, and at the same time the very accurate determination $\gamma=1.3177(5)$ and $\nu=0.6726(8)$ of the critical exponents of the susceptibility and of the correlation length, in the three-dimensional XY universality class, can be achieved. For the exponents at the multicritical $(m, d, N) = (1, 3, 2)$ Lifshitz point the estimates $\gamma_{\parallel}=1.535(25)$, $\nu_{\perp}=0.805(15)$, and $\nu_{\parallel}=0.40(3)$ are obtained. Finally, the susceptibility exponent is estimated along the boundary between the disordered and the modulated phases.

DOI: [10.1103/PhysRevB.78.054405](https://doi.org/10.1103/PhysRevB.78.054405)

PACS number(s): 05.50.+q, 05.70.Jk, 64.60.Kw, 75.10.Hk

I. INTRODUCTION

Bivariate high-temperature (HT) and, in some cases, low-temperature (LT) series expansions have been derived in the last four decades only for very few lattice spin models with interactions extending beyond nearest-neighbor (nn) sites. In principle, undertaking such calculations should be of permanent interest because the analytic approximations based on the series coefficients can make a large part of the (at least) bidimensional interaction-parameter space easily accessible to analysis above (below) the transition temperature. In practice, however, the presence of the next-to-nearest-neighbor (nnn) interactions makes the derivation of adequately long expansions by the conventional graph techniques very laborious. As a consequence, only data at relatively low orders and therefore of limited use have been so far available for a handful of nontrivial models and the less tedious and more flexible approach to the study of these systems by stochastic simulations has largely prevailed in the literature, despite its forced limitation to a coarse-grained survey of the interaction-parameter space and the convergence problems often met within particular regions of the phase diagrams.

The earliest studies of short two-variable¹ (or, in some cases, even three-variable²) series, particularly in the case of N -vector spin systems, helped to substantiate and qualify the critical universality hypothesis in its statement concerning the independence of the critical exponents (and of the other universal quantities) on the range of the interaction. Decisive progress in the study of this property was achieved much later with the advent of simulation algorithms optimized³ for long-range interactions. It was however already known that, when the nnn interactions compete with the nn interactions,

frustration occurs (in absence of disorder) and, as initially shown in the mean-field approximation,^{4,5} produces “special effects.”⁶ The physically interesting new features include the following: (a) the formation of spatially modulated phases, i.e., spin configurations in which the order parameter varies periodically in space with a characteristic modulation wave vector depending on the temperature and the ratio of the competing exchange couplings,^{4–18} and (b) the occurrence of a special multicritical point,⁸ called Lifshitz point (LP), at which the HT disordered phase meets both the LT spatially uniform ordered phase and the LT spatially modulated ordered phase(s).

Competing interactions and LPs are present in a variety of magnetic, ferroelectric, polymeric, liquid crystal systems, in microemulsion models, etc., which sometimes have not yet been studied in complete detail theoretically^{12–21} or experimentally²² and continue to be actively explored. It is also worth mentioning that within the lattice approach to Euclidean quantum-field theory, there is a continuing interest into models of the same or analogous structure,^{23,24} which are expected to show a faster approach to the continuum limit.

II. SPIN MODELS

We begin with a general description of several systems of N -vector spins with nn and nnn interactions on simple-cubic lattices of spatial dimensions $d=1, 2$, and 3 , in zero external field, for which we have computed from the beginning or extended the bivariate HT series. Then we shall discuss a first brief analysis of a small sample of the large body of data

so far accumulated, referring to a particular three-dimensional system of spins with $N=2$ components, i.e., to a classical XY (or planar rotator) model. The case of general N will be the subject of forthcoming work.

We have derived bivariate HT expansions for (i) a class of d -dimensional models with isotropic interactions J_1 among nn spins and isotropic (or anisotropic) interactions J_2 among nnn spins separated by two lattice spacings along $m \leq d$ lattice axes. They are described by the Hamiltonian

$$H_{\text{nnn}}\{v\} = -2J_1 \sum_{\text{nn}} \vec{v}(\vec{r}) \cdot \vec{v}(\vec{r}') - 2J_2 \sum_{\text{nnn}} \vec{v}(\vec{r}) \cdot \vec{v}(\vec{r}'), \quad (1)$$

where we have denoted by $\vec{v}(\vec{r})$ a N -component classical spin vector of unit length situated at the lattice site \vec{r} . In Eq. (1) the first sum, extended to nn spins, describes the interactions among the spin at \vec{r} and the spins at the sites $\vec{r}' = \vec{r} + \hat{x}_i$, with \hat{x}_i a unit lattice vector in the positive x_i direction. The second sum describes the interactions among the spin at \vec{r} and the spins at the sites $\vec{r}' = \vec{r} + 2\hat{x}_i$, with $i = 1, \dots, d$ in the isotropic d -axial case (i.e., in which spins separated by two spacings interact along all lattice axes), whereas i takes only the values $i = d - m + 1, \dots, d$ in the anisotropic m -axial case, with $m < d$. In this paper we study in detail only the most interesting case of the $m=1$ model in $d=3$, which is sometimes denoted also as the three-dimensional ANNNXY model. (ii) A class of models with isotropic or anisotropic interactions J_1 among nn spins and J_2' among (geometric) second-neighbor (sn) spins (sometimes also called $J_1 - J_2$ model or model with crossing bonds) described by the following Hamiltonian:

$$H_{\text{sn}}\{v\} = -2J_1 \sum_{\text{nn}} \vec{v}(\vec{r}) \cdot \vec{v}(\vec{r}') - 2J_2' \sum_{\text{sn}} \vec{v}(\vec{r}) \cdot \vec{v}(\vec{r}'). \quad (2)$$

The first sum in Eq. (2) has the same meaning as in Eq. (1), while the second sum extends to sn spins and describes the coupling of the spin at \vec{r} with the spins at the sites $\vec{r}' = \vec{r} + \hat{x}_i + \hat{x}_j$ and $\vec{r}' = \vec{r} + \hat{x}_i - \hat{x}_j$, with $i < j = 1, \dots, d$ (i.e., the sn interaction acts along the diagonals of the elementary plaquettes).

In Eq. (1) we have denoted by J_1 and J_2 the nn and the nnn exchange interaction constants, respectively. We shall denote by $R = J_2/J_1$ their ratio, which measures the degree of competition of the couplings and therefore is usually called *competition parameter*. In Eq. (2) J_2' denotes the sn interaction constant and we set $R' = J_2'/J_1$. Our HT expansions are expressed in terms of the two variables $K_1 = \beta J_1$ and $K_2 = \beta J_2 (K_2' = \beta J_2')$, with $\beta = 1/kT$, k the Boltzmann constant, and T the temperature.

By the same techniques used in this paper, expansions can be derived also for a much wider variety of systems, but here we shall not be concerned with this possibility. In the case of the *uniaxial* XY model in $d=3$ studied in this paper, our series extends through the 18th order (altogether 171 nonzero coefficients in the case of the susceptibility) the existing²⁵ sixth-order results (21 nonzero coefficients, respectively). The extensions obtained for the other models described in (i) and (ii) are comparable.

The complete set of our series coefficients is too extensive to print here. We shall however upload in the hep-lat archive

a separate report containing a large sample of these data, including the correlation functions between nn and sn (or nnn) spins, the energy density, the susceptibility, and a few correlation moments for the models we have studied.

It is fair to note that, in spite of their high computational complexity and cost, our bivariate series still reach a length which may still be considered only “moderate” with respect to the current best standards for univariate HT expansions. For example, as far as the accuracy of the numerical output of their analysis is concerned, they are not yet comparable with the 25th-order univariate series computed in the case of three-dimensional scalar spin systems with nn interactions²⁶ only (such as the Ising model with generic spin or the lattice Euclidean scalar field) or with the 26th-order series derived²⁷ in the case of the two-dimensional XY model with nn interactions on the square lattice. However, if the comparison is limited to the bivariate series calculated until now for the systems (i) and (ii) (see below), our expansions seem to be already nontrivial enough to justify an update of the few existing HT studies or a first analysis of the data so far unavailable.

We have studied the expansions of observables defined in terms of two-spin correlations, as functions of K_1 at fixed values of R , using, for the moment, only the established *single-variable* methods²⁸ of series analysis, namely, Padé approximants (PAs) or inhomogeneous differential approximants (DAs), and, adopting protocols of analysis well tested in earlier papers,^{25,29-32} we have indeed produced reasonably accurate results which can complement or improve those from different approaches. The choice of single-variable methods of numerical analysis, which might perhaps be considered partly responsible of the limited accuracy of our numerical results, was dictated only by simplicity, but it is likely that now the HT series are long enough to deserve the additional effort of an analysis by tools more powerful and better suited to describe bivariate critical behavior, such as the partial-differential^{28,33} approximants or even some simpler two-variable generalization of PAs.³⁴

For $N > 1$, the lower critical dimension of the so-called (m, d, N) Lifshitz point occurring in a m -axial N -vector system in d dimensions is $d_l(m) = 2 + m/2$, while the upper critical dimension^{8,13} is $d_u(m) = 4 + m/2$. Therefore one has to expect that only in dimension $d > 2$, for the uniaxial model, a LP will show up at $T_{\text{LP}} > 0$ with a nonclassical critical behavior. Thus we can use our HT series for the three-dimensional ANNNXY model to locate its LP and to obtain estimates of its critical exponents, for which some predictions from other approximation methods already exist.

More generally, it is also of interest to analyze the behavior of the series as functions of R all along the critical line separating the paramagnetic from the ordered phases. In particular, along the critical line between the disordered and the ferromagnetic phases we can take advantage in our analysis of the old suggestion^{35,36} that the accuracy in the determination of universal critical parameters of a given N -vector model, such as critical exponents and universal amplitude ratios, can be significantly improved by extending the analysis to a one-parameter family of models belonging to the same universality class. One should then simply “tune” the family parameter in order to minimize or, if possible, to sup-

press the amplitudes of the (nonuniversal) leading nonanalytic corrections to scaling in the observables used to evaluate the critical parameters. This procedure can be implemented by a Monte Carlo (MC) method only,³⁷ by HT-series assisted MC,³⁸ or by HT series only²⁶ and has been successfully applied in a variety of cases involving nn and local spin interactions, so far with a single exception³⁷ for the spin-1/2 Ising model on the simple-cubic lattice. In this case, a high-precision MC analysis showed that turning on an isotropic ferromagnetic coupling beyond nn results into a considerable decrease in the leading correction-to-scaling amplitudes. Unfortunately, this simulation study had to be restricted to a single well-guessed value of the nnn coupling because “tuning” the additional (irrelevant) interaction to search for its best value was too time consuming. Now, in the case of the N -vector model with $N=2$, our expansions are sufficiently extended to produce accurate analytic approximations enabling us to determine in a straightforward way the optimal value of the irrelevant nnn coupling within a fair approximation.

The LP can be located accurately and the exponents of the susceptibility and of the transverse correlation length can be determined with fair precision, while the exponent of the parallel correlation length can be somewhat less accurately estimated. We have also examined the critical behavior of the susceptibility along the branch of the critical line between the disordered and the modulated phases. In this case the results are significantly less accurate and somewhat puzzling: in particular it is not clear whether the transition is (weakly) first order or second order and if this is the case, to which universality class it belongs.

Finally, we can point out another valuable use of our expansions as a guide for possibly more detailed MC investigations of models in the classes (i) and (ii), which might focus on specific points of the parameter space. Even more simply, our expansions can also serve as a realistic test ground for techniques of analysis and resummation of multivariate series. If nothing else, our calculations provide, for a variety of models, an initial set of HT reference data large enough to be a stringent constraint in the validation of future series extensions.

For completeness and in order to put our work into perspective, it is convenient to list the main existing HT results for the systems (i) and (ii) and to mention a few studies related to the subject of this paper but using different techniques. The earliest bivariate HT-series investigation²⁵ of the LP in the N -vector model with nn and uniaxial nnn interactions was mainly devoted to the $N=1$ case (namely, the spin-1/2 Ising model). In three dimensions, series of order 8, 6, and 5 were derived for $N=1, 2$, and 3, respectively. However, only the Ising HT series was considered²⁵ by the authors long enough to yield sufficiently reliable numerical estimates of the location and the exponents of the LP. Both in two and three dimensions, the $N=1$ series were subsequently extended^{29–31} through order 11 for the J_1 - J_2 interaction, for the uniaxial, and for the d -axial interactions. Soon later series for the susceptibility through the 12th order were computed and analyzed³² for uniaxial models on the simple-cubic and the face-centered-cubic lattices. More recently, in two dimensions for the square-lattice Ising model, the susceptibil-

ity expansion was pushed³⁹ through the 13th order for the J_1 - J_2 and the *biaxial* interactions. These have been until now the longest bivariate series derived for systems with nn and nnn interactions.

For the $N \geq 2$ models, on the other hand, there has been no further progress in the HT calculations for the last three decades since the early sixth-order results²⁵ in three dimensions. The only exception to this lack of activity was a study of the biaxial N -vector model (with isotropic nn and nnn interactions on the square lattice), in which the bivariate HT-series-expansion coefficients were computed and tabulated through the fifth order⁴⁰ for *general* values of N . Interest into this model, which constitutes the “Symanzik improved”²³ square-lattice formulation of the $O(N)$ -symmetric nonlinear σ model in two-dimensional Euclidean field theory, came however from quantum-field theorists. In particular, these HT expansions were derived as a means to infer the weak-coupling (i.e., LT) properties of the “improved” nonlinear σ model for $N \geq 3$.

A variety of MC investigations of models with nnn interactions can also be found in the literature: most of them are concerned with the $N=1$ case^{6,30,32,41–45} and some, more directly related to our work, with the $N=2$ case. In particular, the uniaxial XY model in three dimensions was simulated in Refs. 46 and 47, its phase diagram was sketched out, and the location of the LP was estimated along with the exponents of the susceptibility and the magnetization. Later investigations^{48,49} were devoted also to the J_1 - J_2 XY model in two dimensions. These studies were generally limited to only a few points in the interaction-parameter space.

Before a systematic renormalization-group approach could be extended to cover also the class of systems studied here, nontrivial technical difficulties, due to the anisotropy of the scale invariance in the critical behavior at LPs, had to be solved. In particular, while the lowest-order computation of all critical exponents by the ϵ expansion around the LP upper critical dimension $d_u(m)$ [with $\epsilon = d_u(m) - d$] as well as some $O(\epsilon^2)$ results go back to three decades ago,⁸ the extension through second order has been completed^{50,51} only recently. It is encouraging that the $O(\epsilon^2)$ corrections are small and decrease with increasing N , so that a simple truncation to order ϵ^2 of the exponent expansions might already lead to reasonable approximations. Of course, further work is still needed before an accuracy comparable to that established for the usual critical points can be attained.

Results consistent with the $O(\epsilon^2)$ calculations for the exponents of the Ising uniaxial model in three dimensions have also been obtained⁵² from a truncation of the exact renormalization-group equation. Renormalization-group discussions of the ANNNXY model have been given in Refs. 53 and 54.

There has been recent progress⁵⁵ also in the calculation of the leading nontrivial corrections to the large N limit⁵⁶ for some exponents. The layout of the paper is the following: In Sec. II the quantities for which we have computed HT expansions are defined in detail and related to the main critical parameters in particular to the exponents of the uniaxial LP. Section III is devoted to a discussion of the numerical analysis of the series. In Appendix, we briefly describe the non-graphical algorithm used to compute the HT expansions and the checks passed by our series data.

III. HIGH-TEMPERATURE EXPANSIONS

In zero field and for any dimension d , for all models of the classes (i) and (ii) defined on bipartite lattices, the free energy is an even function of J_1 and therefore we can restrict our analyses to the case $J_1 > 0$ (ferromagnetic nn interaction). In general, for $d > 1$ these models exhibit three main phases: a HT paramagnetic (P) phase, a LT uniformly ordered ferromagnetic (F) phase, and a family of LT ordered modulated (M) phases. For $d > 1$, a nontrivial transition line $K_{1c}(R)$ [$K_{1c}(R')$] separates the HT P phase from the LT phases, whereas for $d=1$, one has simply $K_{1c}(R)=\infty$. For $d > d_c(m)$, the critical line $K_{1c}(R)$ is divided into two branches by a LP, a triple point located at a nonzero value $K_{1c}(R_{LP})$ and separating the P - F -transition line from the P - M line.

For $T=0$, the spin ordering can be determined simply by minimizing the energy. The ferromagnetic ground state is energetically favored over the modulated phase(s) only for R greater than some critical value. In the three-dimensional uniaxial case under study, the ground state is made of ferromagnetic layers orthogonal to the z axis, with the relative orientation of the successive layers determined by the value of R .

It is clear that, except in the $d=1$ case, in which the LT region is simply shrunk to the border of the paramagnetic region, the zero-field HT expansions are unsuited to yield much more than hints on the LT structure of the phase diagram and therefore, for the purpose of investigating the LT phases, they have to be replaced by other methods.

For all models of the classes (i) and (ii), we have derived the bivariate expansion of the spin-spin-correlation function,

$$C(\vec{0}, \vec{x}; K_1, R) = \langle \vec{v}(\vec{0}) \cdot \vec{v}(\vec{x}) \rangle, \quad (3)$$

for all values of \vec{x} for which nonvanishing coefficients exist within the maximum order of expansion. The appropriate quantities to be studied in order to locate the P - F branch of the critical line are the ordinary susceptibility,

$$\chi(K_1, R) = 1 + \sum_{\vec{x} \neq 0} \langle \vec{v}(\vec{0}) \cdot \vec{v}(\vec{x}) \rangle, \quad (4)$$

and the l th order spherical moments of the correlation function,

$$m^{(l)}(K_1, R) = \sum_{\vec{x}} |\vec{x}|^l \langle \vec{v}(\vec{0}) \cdot \vec{v}(\vec{x}) \rangle. \quad (5)$$

In terms of $m^{(2)}(K_1, R)$ and $\chi(K_1, R)$, we can construct the correlation length,

$$\xi^2(K_1, R) = m^{(2)}(K_1, R) / 2d\chi(K_1, R). \quad (6)$$

When studying a m -axial model with $m < d$ and therefore with anisotropic interactions, it is convenient to break the d -dimensional lattice vectors \vec{x} as $\vec{x} = (\vec{x}_{\parallel}, \vec{x}_{\perp})$, where \vec{x}_{\parallel} and \vec{x}_{\perp} denote the m -dimensional and the $(d-m)$ -dimensional components of \vec{x} , respectively, parallel and perpendicular to the directions of the nnn interaction.

In order to study the properties of the LP and to locate the P - M transition from the paramagnetic to the LT modulated phase, it is necessary to study also the structure function with respect to \vec{q}_{\parallel}

$$\chi(\vec{q}_{\parallel}; K_1, R) = 1 + \sum_{\vec{x} \neq 0} e^{i\vec{q}_{\parallel} \cdot \vec{x}} \langle \vec{v}(\vec{0}) \cdot \vec{v}(\vec{x}) \rangle \quad (7)$$

and to \vec{q}_{\perp}

$$\chi(\vec{q}_{\perp}; K_1, R) = 1 + \sum_{\vec{x} \neq 0} e^{i\vec{q}_{\perp} \cdot \vec{x}} \langle \vec{v}(\vec{0}) \cdot \vec{v}(\vec{x}) \rangle. \quad (8)$$

In a vicinity of the LP, the scaling behavior of the two-spin-correlation function becomes strongly anisotropic. In particular, the asymptotic behavior for large separation of spins joined by a vector whose components lie entirely in the m -dimensional \vec{x}_{\parallel} subspace differs from the behavior in the case in which the spins are joined by a vector in the $(d-m)$ -dimensional \vec{x}_{\perp} subspace. It is then necessary to replace⁸ each one of the usual correlation exponents η and ν by a pair of exponents associated to the two subspaces. In the first case, the *parallel* correlation exponent is usually denoted by η_{\parallel} (or less frequently, but more suggestively by η_{\parallel}) and in the second case the *transverse* correlation exponent is denoted by η_{\perp} (or by η_{\perp}). Correspondingly, in different directions two distinct correlation lengths ξ_{\parallel} and ξ_{\perp} are observed which diverge with different exponents ν_{\parallel} and ν_{\perp} , respectively. These exponents are related to the susceptibility exponent γ_l at the LP by the ‘‘anisotropic scaling laws,’’

$$\gamma_l = (2 - \eta_{\perp})\nu_{\perp} = (4 - \eta_{\parallel})\nu_{\parallel}. \quad (9)$$

Moreover a generalized hyperscaling law is expected to hold,

$$2 - \alpha_l = m\nu_{\parallel} + (d - m)\nu_{\perp}. \quad (10)$$

The other scaling relations, $\alpha_l + 2\beta_l + \gamma_l = 2$ and $\gamma_l = \beta_l(\delta_l - 1)$, remain unchanged.⁸ We can thus conclude that three independent exponents are requested to characterize the uniaxial LP.

When $d > d_u(m) = 4 + m/2$ and $m = 1$, the critical exponents assume the N -independent mean-field values reported in Table I. In order to estimate the additional critical exponents characterizing a LP, we have also computed the l th order ‘‘parallel moments’’ of the correlation function,

$$m_{\parallel}^{(l)}(K_1, R) = \sum_{\vec{x}} |\vec{x}_{\parallel}|^l \langle \vec{v}(\vec{0}) \cdot \vec{v}(\vec{x}) \rangle, \quad (11)$$

and the l th order ‘‘perpendicular moments,’’

$$m_{\perp}^{(l)}(K_1, R) = \sum_{\vec{x}} |\vec{x}_{\perp}|^l \langle \vec{v}(\vec{0}) \cdot \vec{v}(\vec{x}) \rangle. \quad (12)$$

Near the LP, the correlation length $\xi_{\parallel}^2(K_1, R)$ in a direction within the m -dimensional subspace of the nnn interaction is then expressed in terms of these quantities by

$$\xi_{\parallel}^2(K_1, R_{LP}) = m_{\parallel}^{(2)}(K_1, R_{LP}) / 2m\chi(0; K_1, R_{LP}) \sim \tau(R_{LP})^{-2\nu_{\parallel}} \quad (13)$$

and analogously, the correlation length $\xi_{\perp}^2(K_1, R)$ in a direction orthogonal to the nnn interaction by

TABLE I. Values of the critical exponents for the $(m, d, N) = (1, 3, 2)$ (uniaxial XY) Lifshitz point in three dimensions. The column with heading MF taken from Ref. 50 reports the mean-field exponents. In the column with heading $O(\epsilon^2)$, we report the values obtained (Ref. 50) by evaluating at $\epsilon=3/2$ the ϵ expansions of the exponents truncated at the second order. Under the heading HT we report the results directly obtained in this paper. The heading MC refers to the results of the simulations in Refs. 46 and 47.

Exponent	MF	$O(\epsilon^2)$	HT	MC
γ_l	1	1.495	1.535(25)	1.5(1)
ν_{\parallel}	1/4	0.372	0.40(3)	
ν_{\perp}	1/2	0.757	0.805(15)	
η_{\parallel}	0	-0.020		
η_{\perp}	0	0.042		
α_l	0	-0.047		0.10(14)*
β_l	1/2	0.276		0.20(2)
δ_l	3			
ϕ_l	1/2	0.725	1.00(4)	
β_q	1/2	0.521	0.40(2)	

$$\xi_{\perp}^2(K_1, R_{LP}) = m_{\perp}^{(2)}(K_1, R_{LP})/2(d-m)\chi(0; K_1, R_{LP}) \sim \tau(R_{LP})^{-2\nu_{\perp}}, \quad (14)$$

with $\tau(R) = T/T_c(R) - 1$. Defining, in analogy with $\tau(R_{LP})$, the reduced competition ratio $\rho_{LP} = R/R_{LP} - 1$, a crossover exponent ϕ can be introduced to characterize the behavior of the reduced critical temperature $\tau_{LP} = T_c(R)/T_c(R_{LP}) - 1$ as the LP is approached along the critical line: $\tau_{LP} \sim |\rho_{LP}|^{1/\phi}$. Beside the above exponents, a related⁵⁷ one, $\beta_q = \nu_{\parallel}/\phi$, is associated to the LP. It describes the behavior of the magnitude of the modulation vector \vec{q} as the LP is approached along the branch of the critical line separating the disordered and the modulated ordered phases: $|\vec{q}^2| \sim \rho_{LP}^{2\beta_q}$.

IV. THREE-DIMENSIONAL UNIAXIAL (ANNNXY) MODEL

A. Universality along the P-F branch of the critical line

For R in the range $-1/4 < R < \infty$, the ground state of the system is ferromagnetic and the uniform ferromagnetic ordering persists at $T > 0$ up to some inverse temperature $K_{1c}(R)$, at which a second-order phase transition, expected to belong to the universality class of the three-dimensional XY model, occurs between the LT phase and the HT paramagnetic phase. In this section we shall mainly discuss the numerical evidence obtained from the analysis of our HT series that, in the ferromagnetic range of R , this transition actually belongs to the XY universality class. We shall then argue that, if this is the case, the parameter R can be exploited to determine very accurate values of the critical exponents for the XY universality class.

For each value of R , we can locate the transition by analyzing the HT expansion of the ordinary susceptibility $\chi(K_1, R)$, whose coefficients show generally a smooth dependence on the order of expansion and a fast approach to their

asymptotic forms and thus are well suited to numerical study. The critical behavior of the susceptibility as $\tau(R) \rightarrow 0^+$ is expected to be

$$\chi(K_1, R) = A_{\chi}^+(R)\tau(R)^{-\gamma(R)}\{1 + a_{\chi}^+(R)\tau(R)^{\omega(R)} + O[\tau(R)]\}, \quad (15)$$

where $A_{\chi}^+(R)$ is the critical amplitude of the susceptibility and $a_{\chi}^+(R)$ is the leading correction-to-scaling amplitude. We have denoted $\gamma(R)$ and $\omega(R)$ as *a priori* R dependent, although we shall finally argue that, as expected, they are universal with respect to R , namely, independent of R .

The critical behavior of the second-moment correlation length may analogously be characterized as

$$\xi^2(K_1, R) = A_{\xi}^+(R)\tau(R)^{-2\nu(R)}\{1 + a_{\xi}^+(R)\tau(R)^{\omega(R)} + O[\tau(R)]\}. \quad (16)$$

We shall resum the susceptibility series by inhomogeneous second-order DAs in the variable K_1 at fixed R . In this and in the analyses that follow, we have used a set of quasi-diagonal DAs chosen as the approximants $[k, l, m; n]$ with $14 \leq k+l+m+n \leq 16$, namely, those using not less than 17 series coefficients. We have taken $|k-l|$, $|l-m|$, and $|k-m| < 3$ with $k, l, m > 3$, while $1 \leq n \leq 4$. We have however always made sure that our numerical estimates depend only weakly on this choice. The results for the critical line obtained in this way (for $R_{LP} \leq R \leq 2$) are reported in Fig. 1. Note that we have preferred to plot vs R the quantity $T_c(R)/2 = 1/2K_{1c}(R)$ rather than $K_{1c}(R)$ itself, in order to make our figure immediately comparable with the figure, covering a smaller range of R , which appears in the MC study in Ref. 46. On the scale in Fig. 1, the three data points $[R=0, T_c(R)/2=2.17(2)]$, $[R=-0.25, T_c(R)/2=1.83(2)]$, and $[R=-0.26, T_c(R)/2=1.82(2)]$ obtained⁴⁶ in the MC study are hardly distinguishable from our curve. The corresponding values determined by our series are $[R=0, T_c(R)/2=2.2017(2)]$, $[R=-0.25, T_c(R)/2=1.830(1)]$, and $[R=-0.26, T_c(R)/2=1.809(1)]$. Our result at $R=0$ compares well with the estimate $[R=0, T_c(R)/2=2.20172(15)]$, obtained⁵⁸ by 21st-order HT expansions. Note also that the spreads $\delta K_{1c}(R)$ of our DA estimates of the critical temperatures, which are smaller than those of the MC study by one order of magnitude, are invisible on the scale of the figure. For convenience, we have listed in Table II few numerical values of $K_{1c}(R)$.

It should be stressed that it is generally difficult to assess very accurately the real uncertainties of the results in this kind of analysis mainly because, due to the finite (and in our case still moderate) length of the series, the sequences of DA estimates may retain residual trends which call for further extrapolation, particularly so for $R \geq 1$. Whenever possible, one should then try to infer the size of the uncertainties also from a comparison with the results of approximation procedures alternative to the direct DA calculation and thus presumably having different convergence rates and different mechanisms of error buildup. In our case, we shall eventually argue that the spreads of the DA estimates of the critical

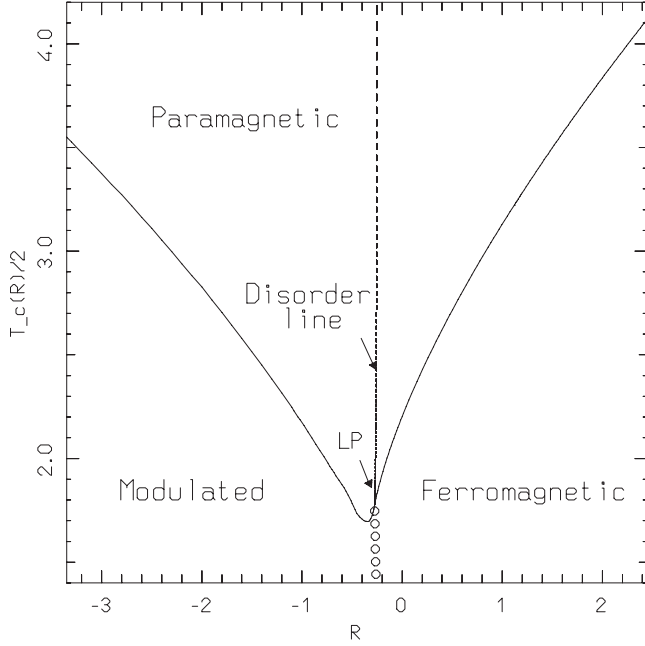


FIG. 1. The phase diagram of the three-dimensional uniaxial XY model. In the $[R, T_c(R)]$ plane, we have represented by a continuous line the locus of critical points separating the disordered (paramagnetic) phase from the ordered (ferromagnetic and modulated) phases. In the scale of the figure, the uncertainties of the points are smaller than the width of the line. The Lifshitz point (LP) is located at the intersection of the critical and the disorder line (represented by a dashed curve). A transition line, also expected to be of second order, separates the modulated from the ferromagnetic phase and joins the Lifshitz point to the point $(R=-1/4, T=0)$, where the ordering of the ground-state changes. This line cannot be mapped out by HT methods and therefore is only schematically indicated by a sequence of open circles.

temperature, already at these orders of HT expansion, are reasonable approximations of the uncertainties, at least for positive and not too large R .

Let us then consider an example of an alternative approach to the determination of $K_{1c}(R)$. If the critical singularity is the nearest singularity, we can determine it also by evaluating the limit of the sequence of estimators $[K_{1c}(R)]_n$ of $K_{1c}(R)$ defined by the modified-ratio prescription,^{28,35}

$$[K_{1c}(R)]_n = \left(\frac{c_{n-2}c_{n-3}}{c_n c_{n-1}} \right)^{1/4} \exp \left[\frac{s_n + s_{n-2}}{2s_n(s_n - s_{n-2})} \right], \quad (17)$$

where

$$s_n = \left[\ln \left(\frac{c_{n-2}^2}{c_n c_{n-4}} \right)^{-1} + \ln \left(\frac{c_{n-3}^2}{c_{n-1} c_{n-5}} \right)^{-1} \right] / 2 \quad (18)$$

and $c_n(R)$ are the HT expansion coefficients of the susceptibility.

This prescription has the important advantage of bringing information not only about $K_{1c}(R)$ but also on the leading correction-to-scaling amplitude $a_\chi^+(R)$, defined by Eq. (15), a quantity which in general rules the convergence properties of any approximation method in the critical region. Indeed, we have observed²⁶ that the modified-ratio sequence has the

TABLE II. The critical values of K_1 for selected values of R . The uncertainties reported here correspond only to the spread of the DA estimates and therefore are likely to underestimate the real errors when $|R-R_M|$ is not small, particularly so for $R \leq 0$.

R	$K_{1c}(R)$
1.200	0.152 39(4)
1.100	0.155 96(4)
1.000	0.159 80(4)
0.900	0.163 91(3)
0.800	0.168 36(3)
0.700	0.173 19(2)
0.600	0.178 47(2)
0.500	0.184 29(1)
0.400	0.190 75(1)
0.300	0.197 99(1)
0.200	0.206 23(1)
0.100	0.215 77(1)
0.000	0.227 10(2)
-0.100	0.241 13(4)

simple asymptotic behavior for large order n ,

$$[K_{1c}(R)]_n = K_{1c}(R) \left(1 - \frac{C(\gamma, \omega) a_\chi^+(R)}{n^{1+\omega}} + O(1/n^2) \right), \quad (19)$$

where $C(\gamma, \omega)$ is some known positive function of γ and ω .

In order to use effectively the modified-ratio method, we shall now *assume* that the exponent $\omega = \omega(R)$ of the leading correction to scaling is independent of R and takes the value⁵⁸ $\omega \approx 0.52$ (an assumption which was not necessary to make in the DA method discussion). Then by fitting the sequence $[K_{1c}(R)]_n$ to the simple form $b_1(R) - b_2(R)/n^{1+\omega}$, we can estimate the amplitude $a_\chi^+(R)$ from the value of the parameter $b_2(R)$. Although rather long and smooth series are usually necessary²⁶ to obtain accurate estimates by this method, we can observe a complete consistency between the estimates of $K_{1c}(R)$ from the DAs and the values of $b_1(R)$ obtained by the fit (within a small multiple of their spreads for positive and not too large R), so that the results cannot be distinguished from those reported in Fig. 1. This fact also gives support to our simple fit procedure for determining $b_2(R)$ and, at the same time, it suggests that the spread of the DA estimates of the critical temperatures might be taken as a sound measure of their real uncertainties. In order to illustrate our fit procedure for determining $b_2(R)$, in Fig. 2 we have plotted vs $x=1/n^{1+\omega}$ the sequence of modified ratios $[K_{1c}(R)]_n$ normalized to their extrapolated values $b_1(R)$, for a few fixed values of R , chosen in a vicinity of R_M . Let us add that only for $R \geq 0$ the sequences $[K_{1c}(R)]_n$ are sufficiently smooth that these rough, but sufficiently reliable, estimates of $b_2(R)$ are feasible, while unfortunately for $R < 0$ the modified-ratio sequences develop strong oscillations and a straightforward two-parameter fit cannot work. The important observation now is that the function $b_2(R)$ vanishes at $R=R_M \approx 0.28(3)$ and therefore its absolute value is minimum

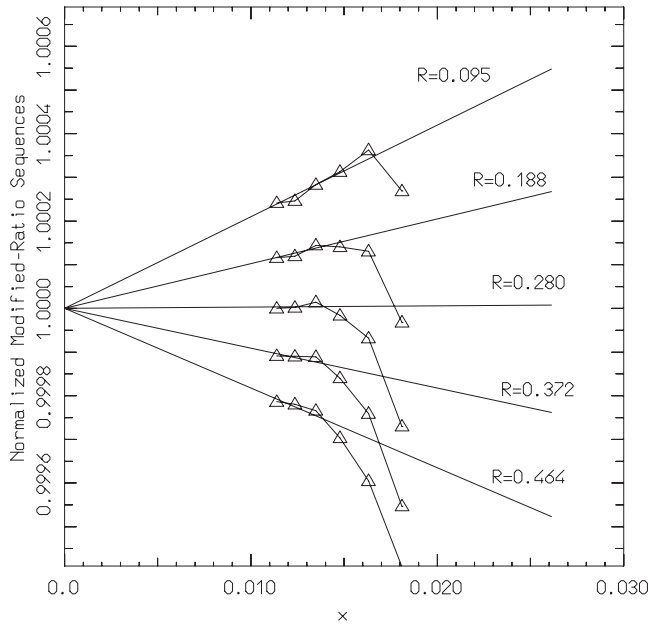


FIG. 2. A representation of the modified-ratio sequences $[K_{1c}(R)]_n$ obtained from Eq. (17). For a few values of R chosen in a vicinity of R_M , the sequences have been extrapolated to large order by fitting them to the asymptotic form $b_1(R) - b_2(R)/n^{1+\omega}$, with $\omega=0.52$. We have then plotted the modified-ratio sequences vs $x=1/n^{1+\omega}$ after normalizing them to their limiting values $b_1(R)$. The elements of the normalized sequences are represented by open triangles and are connected by continuous lines as a guide for the eyes. The corresponding best fits to the asymptotic form, $1 - a(R)/n^{1+\omega}$ with $a(R)=b_2(R)/b_1(R)$, are represented by straight continuous lines.

at this point. From our estimates of $b_2(R)$, we can infer the sign and size of the deviations from the exact values which should be expected for the central DA estimates of $K_{1c}(R)$ and of the exponents as R varies. More precisely, we have to expect⁵⁹ that, in the range $R > R_M$, where $b_2(R)$ and therefore $a_\chi^+(R)$ are found to be positive, the critical inverse temperatures and the critical exponents will be underestimated by our analyses, while the opposite will be observed for $R < R_M$. This is clear from Eq. (19) as far as the critical inverse temperatures are concerned. In order to reach the same conclusion for the exponents, one may either use an asymptotic formula²⁶ analogous to Eq. (19) or consider that in approximate calculations some effective exponent⁵⁹ is generally evaluated, for example, $\gamma_{\text{eff}}(\bar{\tau}) = -\frac{d \log(\chi)}{d \log(\bar{\tau})} \simeq \gamma - \omega a_\chi^+ \bar{\tau}^\omega$, with $\bar{\tau}$ small but nonzero. In order to relate these remarks to the behavior of $b_2(R)$, the absolute value of $b_2(R)$, obtained from a fit of the four highest-order estimators $[K_{1c}(R)]_n$ in the modified-ratio sequence, is very schematically plotted vs R , together with the exponent estimates, in Fig. 3 and in some of the following figures. All previous considerations also apply to the study of the HT expansion of $\xi^2(K_1, R)$.

In Fig. 3, the critical exponents $\gamma(R)$ of the susceptibility and $\nu_\perp(R)$ of the transverse correlation length [note that $\nu_\perp(R)$ and $\nu_\parallel(R)$ coincide with $\nu(R)$ for $R \geq 0$] are plotted as functions of R along the P - F branch of the critical line. They have been computed both using second-order DAs biased

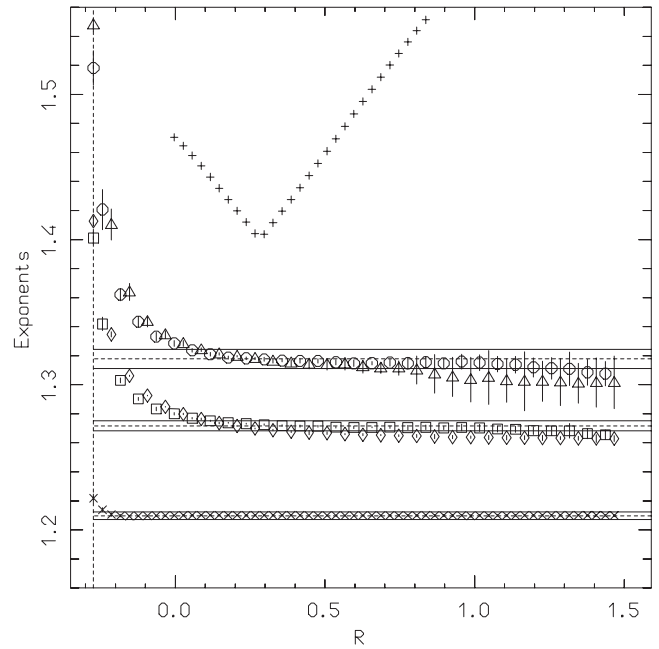


FIG. 3. The exponents $\gamma(R)$ and $\nu_\perp(R)$ (note that for $R \geq 0$ $\nu_\perp = \nu$) are computed along the P - F branch of the critical line $K_{1c} = K_{1c}(R)$ in order to display their universality with respect to R . The horizontal continuous lines are bands of 0.5% deviation from the central values, indicated by dashed lines, of recent high-precision estimates (Ref. 38) of the exponents γ (in the case of the upper band), ν (central band, shifted upward by 0.6), and of the ratio ν/γ (lower band shifted upward by 0.7) for the XY universality class. We have indicated by open circles our estimates of the exponent $\gamma(R)$ obtained from DAs biased with the critical temperature, while the estimates obtained by the critical-point renormalization method, generally subject to a larger uncertainty, are denoted by open triangles. In the case of the exponent $\nu_\perp(R)$ we have denoted by open rhombs the estimates obtained from DAs biased with the critical temperature and by open squares the estimates obtained by the critical-point renormalization method. As already noted, for graphical convenience, the values of this exponent are shifted upward by 0.6. Finally a sequence of stars denotes the ratios $\nu_\perp(R)/\gamma(R)$ which, again for convenience, are shifted upward by 0.7. A sequence of crosses schematically indicates a quantity proportional to the absolute value $|a_\chi^+(R)|$ of the correction-to-scaling amplitude. For graphical convenience, this quantity is shifted upward by 1.4. The vertical dashed line on the left-hand side indicates the value $R_{LP} = -0.2733(5)$ corresponding to the LP.

with the critical singularity $K_{1c}(R)$ and, alternatively, also by the method of “critical-point renormalization.”⁶⁰ The latter method consists in analyzing the term-by-term divided series $W(x, R) = \sum_s d_s(R)/c_s(R)x^s$, where $d_s(R)$ are the expansion coefficients of $\chi^2(K_1, R)$ [or of $\xi^4(K_1, R)/K_1^2$] and $c_s(R)$ are the coefficients of $\chi(K_1, R)$ [or of $\xi^2(K_1, R)/K_1$]. It can be shown that if the nearest singularity is the critical point, then $W(x, R)$ is singular at $x=1$ with an exponent $-[1 + \gamma(R)]$ $\{-[1 + 2\nu(R)]\}$, which can be estimated by forming DAs of $W(x, R)$ biased to be singular at $x=1$. This alternative determination of the exponents is of particular interest in the ranges of values of R in which the accuracy of the available estimates of $K_{1c}(R)$ might be insufficient to obtain good temperature-biased estimates or where the convergence of

the DAs is slow. It is not surprising that in a neighborhood of R_M (where the amplitude of the leading correction to scaling is vanishing), this method and the direct analysis of the susceptibility (or of the correlation length) by temperature-biased DAs yield essentially the same exponent estimates, while elsewhere they show some small difference. In Fig. 3, the results of both approximations are plotted vs R and compared with a recent high-accuracy determination³⁸ $\gamma=1.3178(2)$ and $\nu=0.671\,55(27)$ of the exponents γ and ν for the XY universality class. Our two approximations for $\gamma(R)$ and $\nu(R)$ show a similar behavior: for $R > R_M$ both lead to estimates slightly smaller than the data chosen for comparison, while the opposite happens for $R < R_M$. This is precisely what can be anticipated from our determination of the leading correction-to-scaling amplitude. Overall, as shown in Fig. 3, for $0.1 \leq R \leq 1$, the central values of our estimates of the critical exponents deviate from the estimates at $R=R_M$ by less than 0.5%, while in the wider range $0 \leq R \leq 1.5$ the deviations do not exceed 1%, thus indicating that our approximate results have a very weak dependence on R to within a fair accuracy. Even more accurate results are obtained computing, for example, by *simplified*⁶¹ DAs [biased with $K_{1c}(R)$ and with the correction-to-scaling exponent ω], the ratio of the logarithmic derivatives of the quantities $m_{\perp}^{(2)}(K_1, R)/K_1$ and $\chi(K_1, R)$, which yields the ratio $\nu_{\perp}(R)/\gamma(R)$. As it is also shown in Fig. 3, the estimates so obtained for this ratio appear to be independent of R to within 0.1% along the whole interval $0 \leq R \leq 1.5$, in which they remain quite near to the ratio of the data³⁸ chosen for comparison. Of course, this particularly favorable result is simply due to the fact that the relative deviations of $\gamma(R)$ and $\nu_{\perp}(R)$, with respect to their values at R_M , keep the same sign and a similar size as R varies.

A blown-up view of part of these results is presented in Fig. 4, where we have plotted our temperature-biased DA estimates of the exponents $\gamma(R)$, $\nu_{\perp}(R)$ and of their ratio, after normalizing them to the corresponding comparison³⁸ values. It is amusing to remark that, for positive and not too large values of R , our rough determination of the behavior of $a_{\chi}(R)$ also suggests a simple prescription to improve the estimates of the exponents by temperature-biased DAs. We have to simply correct for the expected errors in the bias values of $K_{1c}(R)$, computing the critical exponents by DAs biased with $K_{1c}(R) + \delta K_{1c}(R)/2$ when $R > R_M + 0.03$ or with $K_{1c}(R) - \delta K_{1c}(R)/2$ when $R < R_M - 0.03$. We have shown in Fig. 5 that this quite naive adjustment of the standard biasing procedure to account for the sign and size of $a_{\chi}(R)$ improves visibly the universality of the exponents with respect to R . At the same time, this result gives further support to our conjecture that the spread $\delta K_{1c}(R)$ of the DA estimates of $K_{1c}(R)$ is a sound approximation of their uncertainty, provided that R is positive and not too large.

We have also studied other indicators of universality, such as, for example, the values at the critical point $K_{1c}(R)$ of the correlation-moment ratios,

$$Q(p, q; r, s; R) = \frac{m^{(p)}(K_1, R)m^{(q)}(K_1, R)}{m^{(r)}(K_1, R)m^{(s)}(K_1, R)}, \quad (20)$$

with $p+q=r+s$. As expected, they show an approximate independence on R for $R > 0$. This is shown in Fig. 6, where

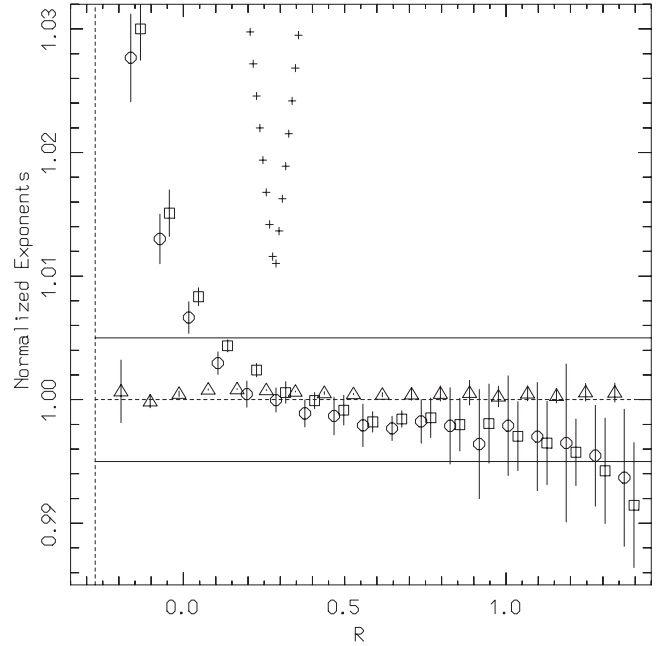


FIG. 4. A slightly modified and blown-up representation of some of the data appearing in Fig. 3. We report the exponents $\gamma(R)$ (open circles), $\nu_{\perp}(R)$ (open squares), and the ratio $\nu_{\perp}(R)/\gamma(R)$ (open triangles) computed by temperature-biased DAs along the P - F branch of the critical line $K_{1c}=K_{1c}(R)$. The data are now normalized to the central values of the corresponding comparison estimates (Ref. 38) of the exponents for the XY universality class. The horizontal solid lines are bands of 0.5% deviation from the comparison value (central dashed line). The vertical dashed line on the left-hand side indicates the value of R_{LP} . The upper curve, schematically denoted by crosses, plots a quantity proportional to the absolute value $|a_{\chi}^{+}(R)|$ of the correction-to-scaling amplitude. This quantity is shifted upward by 1.01 for graphical convenience.

we have plotted vs R a few ratios $Q(p, q; r, s; R)$ evaluated at the critical point and normalized to their value $Q(p, q; r, s; R_M)$ at R_M . Our estimates refer to the cases in which $(q=p=1/2; r=1/4, s=3/4)$, $(q=1/2, p=1/4; r=0, s=3/4)$, or $(q=p=1/2; r=0, s=1)$.

As long as R is positive and not too large, we can conclude that all these results consistently and rather convincingly indicate that, along the P - F branch of the critical line, the small violations of the exponent universality with respect to R , shown by our numerical computations, are only apparent and can be entirely ascribed to the slow convergence of approximation procedures still unable, at the present orders of expansion, to account fully for the presence of corrections to scaling.

These evidences of universality with respect to R justify the technique^{35,36} that we can adopt in order to improve the accuracy in the determination of the exponents for the XY universality class. We can observe that, as R varies in the ferromagnetic range, we have an R -dependent family of models all of which can be assumed to belong to the XY universality class, so that they share the same critical exponents, while they have generally different R -dependent (namely, nonuniversal) amplitudes of the corrections to scaling. Therefore, we expect that the best approximations for

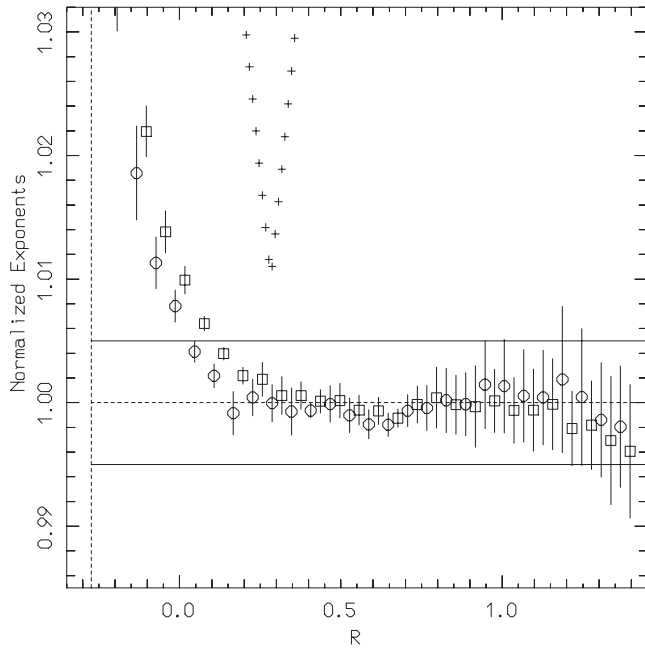


FIG. 5. Same as Fig. 4, but here the exponents $\gamma(R)$ (open circles) and $\nu_{\perp}(R)$ (open squares) are computed along the P - F branch of the critical line by DAs biased with $K_{1c}(R) + \delta K_{1c}(R)/2$ for $R > R_M + 0.03$ or biased with $K_{1c}(R) - \delta K_{1c}(R)/2$ for $R < R_M - 0.03$. Like in Fig. 4, the exponents are normalized to the mentioned (Ref. 38) comparison central values $\gamma = 1.3178$ and $\nu = 0.6717$, respectively. The horizontal solid lines are bands of 0.5% deviation from the central value indicated by a dashed line. The vertical dashed line indicates the value of R_{LP} . The sequence of crosses represents a quantity proportional to the absolute value $|a_{\chi}^+(R)|$ of the correction-to-scaling amplitude (shifted upward by 1.01 for graphical convenience).

the universal quantities will be achieved from the study of the model with $R = R_M$ because $a_{\chi}^+(R_M)$ vanishes. For this particular model in the family also the other leading correction amplitudes of interest, for example, $a_{\xi^2}^+(R)$, must vanish at R_M , since the correction-amplitude ratios such as $a_{\chi}^+(R)/a_{\xi^2}^+(R)$ are universal.

These arguments support our belief that our exponent estimates $\gamma(R_M) = 1.3177(5)$, $\nu(R_M) = 0.6726(8)$, and $\nu(R_M)/\gamma(R_M) = 0.5100(1)$ should be rated as the best possible determinations of the susceptibility and correlation-length exponents in the XY universality class, which one can extract, at the present expansion order, from our R -dependent family of HT series. The high-precision estimates³⁸ of the XY universality class exponents that we have compared with our results in Fig. 3 were also obtained using a similar improvement procedure in the case of a different family of nn-interaction models for which series of order 23 are known. Our best estimate of the susceptibility exponent agrees well with the corresponding result cited for comparison, although the uncertainty of our result is sizably larger due to the still moderate length of our bivariate series. On the other hand, the central value of our best estimate for the exponent ν is somewhat larger than [while the estimate $\nu = 0.6720(4)$ obtained from those of γ and of the ratio ν/γ is much closer to] the corresponding comparison value. Our direct estimate of ν

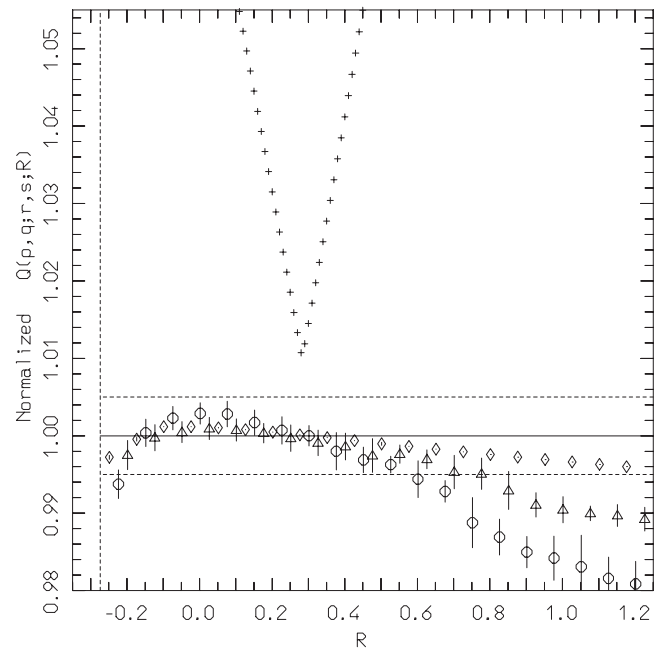


FIG. 6. Universality with respect to R of the moment ratios $Q(p, q; r, s; R)$. We have reported results for $Q(1/2, 1/2; 0, 1; R)$ represented by circles for $Q(1/2, 1/4; 0, 3/4; R)$ (triangles) and for $Q(1/2, 1/2; 1/4, 3/4; R)$ (rhombs). The ratios are normalized to their values at R_M . The values of these ratios at R_M are $Q(1/2, 1/2; 0, 1; R_M) = 0.876(1)$, $Q(1/2, 1/4; 0, 3/4; R_M) = 0.929(1)$, and $Q(1/2, 1/2; 1/4, 3/4; R_M) = 0.9695(1)$. The sequence of crosses represents a quantity proportional to the absolute value $|a_{\chi}^+(R)|$ of the correction-to-scaling amplitude (and is shifted upward by 1.01 for graphical convenience). The vertical dashed line indicates the value of R_{LP} .

is closer to the older MC result⁶² $\nu = 0.6723(3)$ (Ref. 8) and to the result $\nu = 0.6717(3)$ of the simulation in Refs. 63 and 64. It is, however, much larger than the value $\nu = 0.6709(1)$ obtained, by using the hyperscaling relation $2 - \alpha = d\nu$, from the recent high-accuracy measure $\alpha = 0.0127(3)$ of the ⁴He specific heat in a microgravity experiment.⁶⁵

In Ref. 63 recent determinations of ν with increasing accuracy have been summarized into a useful diagram showing that the central estimates from the most recent MC simulations and HT-series analyses are, in general, significantly larger than those obtained both from the renormalization group and from the cited experimental measure. This is an interesting remark which calls, at least, for a more accurate reassessment of the uncertainties of the results in the literature. As far as our HT approach is concerned, we can reasonably expect that an extension of the bivariate expansions by only a couple of orders would significantly reduce the uncertainties of our best estimates of the exponents, particularly so for the direct estimate of ν . Presently, however, it might be less difficult to give further support to our arguments and make them sharper by using our series results as a guide for a high-precision MC simulation of the ANNNXY model at $R = R_M$.

Finally we must add that, unfortunately, our series for the specific heat, which is a very weakly singular quantity, seems to be still insufficiently long to yield an evaluation of

comparable accuracy for the exponent $\alpha(R)$. We can only infer that on the P - F line, $\alpha(R) \approx -0.01(2)$, as expected. This result is completely compatible with the bounds $-0.0202 < \alpha < -0.0124$ obtained introducing into the hyperscaling relation the extreme values of the range of estimates of ν reported in the recent literature. We can conclude our study of the critical behavior along the P - F line remarking that from a study of $T_c(R)$ in a vicinity of T_{LP} , we can estimate $\phi = 1.00(4)$, since it appears that the curve $T_c = T_c(R)$ changes from concave to convex in a small vicinity of $T(R_{LP})$.

B. Lifshitz point and the P - M branch of the critical line

In the mean-field approximation $R_{LP} = -1/4$, but our HT calculation shifts this value by $\approx 10\%$ to the modulated side of the phase diagram. For $R_{LP} < R \leq 0$, the critical exponents crossover⁶⁶ from the value of the XY universality class to the LP critical behavior. In this range of R , the amplitudes $a_\chi^+(R)$ and $a_\xi^+(R)$ appearing in Eqs. (15) and (16) lose their leading role because also higher-order correction amplitudes become important, the convergence of our series slows down and they appear inadequate to exhibit the universality with respect to R of the exponents and their expected discontinuous change to the values of the LP universality class at $R = R_{LP}$. Thus, of course, in the crossover region, also the spreads of our estimates will grossly underestimate the real errors.

Let us now recall that the equation $m_\parallel^{(2)}(K_1, R) = 0$ implicitly defines in the R - T plane the so-called *disorder* line,⁷ which, within the paramagnetic phase, divides a region with monotonically (exponentially) decaying correlations along the direction parallel to the nnn interaction from a region with oscillating but still exponentially damped correlations. The equation defining the disorder line can be solved iteratively with respect to R to form the single-variable series $R_{dis} = R_{dis}(T)$, which finally is resummed by DAs. The plot of the disorder line obtained from this series is drawn as an almost vertical dashed line in Fig. 1. It may be of interest to show how accurately the spin-spin correlations can be computed at HT and therefore we have displayed in Fig. 7 the qualitative difference in their behavior as functions of the distance of the spins along the z direction on the two sides of the disorder line. Using our knowledge of the spin-spin correlations, we can also show that the LT modulated order already begins to build up in the nearly critical HT phase. This is suggested by Fig. 8, where we have plotted vs R the values of the energy, the nn and the nnn spin correlations along the z axis, calculated just above the boundary of the paramagnetic phase, precisely at $T = 1.1T_c(R)$. We can observe that the energy reaches a maximum near R_{LP} , where the disorder is higher and that the nn spins are positively correlated on the whole range of R (albeit not too strongly since T is high). On the other hand the nnn spins tend to be more correlated than the nn spins for $R \geq 1.2$, while as R is lowered, this correlation decays to become negative when $R \leq R_{LP}$.

In order to locate the LP on the boundary of the paramagnetic phase, we have to recall^{25,32} that for small q_z

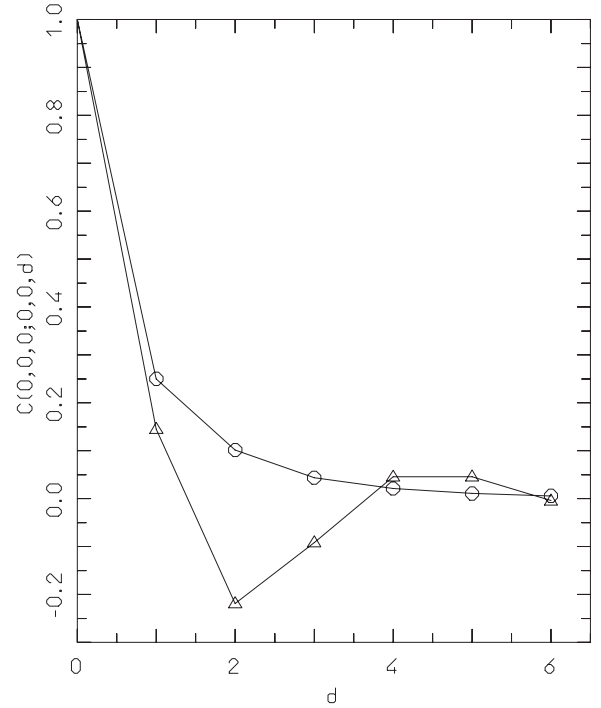


FIG. 7. The correlation function $C(0,0,0;0,0,d)$ between the spin at the origin and a spin on the z axis as a function of the distance d between the spins at fixed values of R and T . We have chosen the value $[R=0.11, T_c(R)/2=2.59]$ (open circles) on the right hand of the disorder line and the value $[R=-1.0, T_c(R)/2=2.439]$ (open triangles) on the left hand of it to display the different behavior of the corresponding correlation function (pure exponential decay and oscillating exponential decay, respectively). The lines connecting the symbols are drawn as a guide for the eyes.

$$\begin{aligned} & \chi(0, K_1, R) / \chi(q_z, K_1, R) \\ &= 1 + q_z^2 \frac{m_\parallel^{(2)}(K_1, R)}{2\chi(K_1, R)} + q_z^4 \left(\frac{m_\parallel^{(2)}(K_1, R)^2}{4\chi(K_1, R)^2} - \frac{m_\parallel^{(4)}(K_1, R)}{24\chi(K_1, R)} \right) \\ &+ \dots, \end{aligned} \tag{21}$$

showing that the minimum at $q_z=0$, which characterizes $\chi(0, K_1, R) / \chi(q_z, K_1, R)$ at fixed K_1 , when R is in the ferromagnetic range, changes to a local maximum as $R \rightarrow R_{dis}(K_1)$ where the second-order parallel moment $m_\parallel^{(2)}(K_1, R) = 0$. Thus the LP is found at the intersection of the P - F branch of the critical line with the disorder line. Following this procedure we are led to the estimate $(R_{LP} = -0.2733(6) \text{ and } T(R_{LP}) = 1.778(2))$ of the intersection point between the critical locus and the disorder line. The value of R_{LP} obtained in this way is consistent with that obtained minimizing $\chi(0, K_1, R) / \chi(q_z, K_1, R)$ with respect to q_z^2 as $R - R_{LP} \rightarrow 0^-$ and $K_1 \rightarrow K_1(R)$. Indeed, for small q_z^2 , we obtain from Eq. (21) that the position of the minimum \bar{q}_z^2 vs R is given by

$$\bar{q}_z^2 \approx \frac{6m_\parallel^{(2)}(K_1, R)\chi(K_1, R)}{m_\parallel^{(4)}(K_1, R)\chi(K_1, R) - 6m_\parallel^{(2)}(K_1, R)^2} \tag{22}$$

evaluated at the critical point $K_{1c} = K_{1c}(R)$ for $R \leq R_{LP}$. By resumming the series expansion of \bar{q}_z^2 , we can determine R_{LP} also as the value of R at which $\bar{q}_z^2 = 0$.

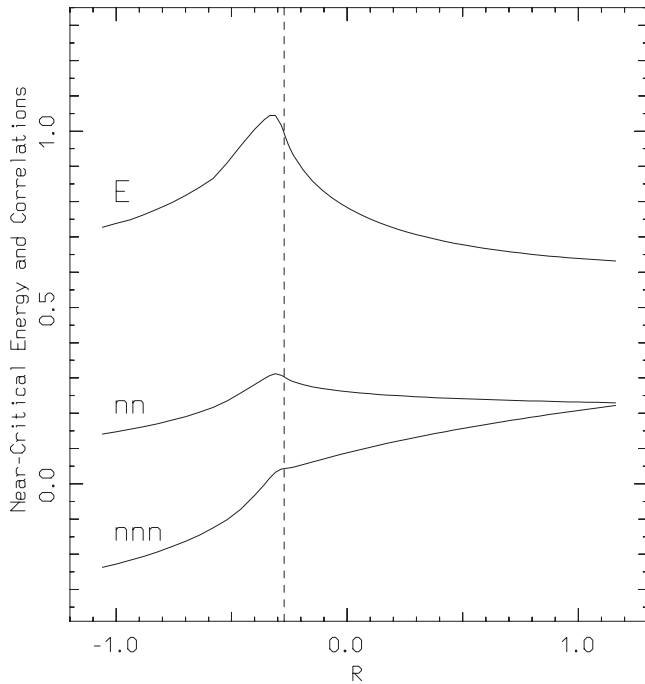


FIG. 8. The energy (upper curve), the nn-spin-correlation function (middle curve), and the nnn-spin-correlation function (lowest curve) computed near the boundary of the paramagnetic phase [at $T = 1.1T_c(R)$] and plotted vs R . The vertical dashed line indicates the value of R_{LP} .

For $R \leq 0$, in the crossover region, Figs. 3 and 9 show a steep rise of our exponent estimates near the LP and past it, followed by a somewhat slower decay extending through $R \approx -0.8$. A completely similar behavior of the exponent $\gamma(R)$ nearby the LP was noted in a HT study³² of the 3d Ising uniaxial model. In this study, we should then assume that the values of the exponents at the LP are not strongly affected by the crossover and also be aware that they are rather sensitive to the location of the LP. Using the critical-point renormalization method, we can estimate $\gamma_l = 1.55(1)$, while the biased DAs suggest $\gamma_l = 1.52(1)$, as shown in Fig. 3. We shall take a weighted average of these values as our final estimate of the exponent, $\gamma_l = 1.535 \pm 0.025 \pm 0.2|R_{LP} + 0.2733|$, including explicitly in our error a contribution from the uncertainty of R_{LP} . This result has a smaller uncertainty but is completely compatible with the estimate $\gamma_l = 1.5(1)$ of the MC simulation in Ref. 47. Note that our estimates of R_{LP} and $T(R_{LP})/2$ differ by $\approx 5\%$ from the values $R_{LP} = -0.263(2)$ and $T_{LP}(R)/2. \approx 1.82$, determined by the old (sixth-order) series²⁵ and used as an input in the MC (Refs. 46 and 47) study. Our estimate of the exponent is also not far from the value $\gamma_l = 1.495$ obtained^{50,55} simply by setting $\epsilon = d_u(1) - d = 3/2$ in the two-loop ϵ expansion.

Starting with the HT expansions of $\xi_{\perp}^2(K_1, R)$, similar considerations yield the estimate $\nu_{\perp} = 0.805 \pm 0.015 \pm 0.1|R_{LP} + 0.2733|$. For this exponent, no MC results are available and our result can be compared only with the value $\nu_{\perp} = 0.757$ from the ϵ expansion.

The direct estimate of ν_{\parallel} from the analysis of ξ_{\parallel} is notoriously difficult because, in the P phase near the Lifshitz point, the competition between the nn and the nnn interaction

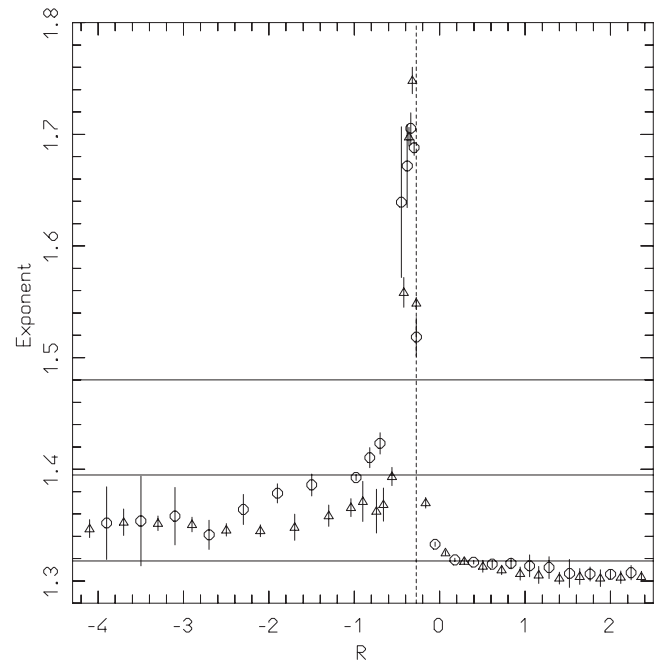


FIG. 9. The exponent $\gamma(R)$ computed along the P - M branch of the critical line. The estimates obtained by the critical-point renormalization method are represented as open triangles, those obtained by DAs biased with the critical temperature as open circles. The horizontal continuous lines represent the values of the exponent γ for the $O(2)$ (lowest line), $O(3)$ (intermediate line), and $O(4)$ (upper line) universality classes. The vertical dashed line indicates the value of R_{LP} .

reduces drastically the correlation length in the z direction. In particular, in the $N=1$ case, the determination of ν_{\parallel} has so far eluded even the most extensive⁴⁵ MC simulation so far available. In the large N limit (namely, in the case of the uniaxial spherical model), in which very long HT expansions can be easily computed, it was observed²⁵ that at least 35 orders are necessary to approximate the behavior of ξ_{\parallel} . Also in the $N=2$ case under study, the length of our HT expansions, unfortunately, seems to be still insufficient. We can, however, try to estimate indirectly ν_{\parallel} either from a measure of the exponents β_q and ϕ , taking advantage of the scaling law $\nu_{\parallel} = \beta_q \phi$, or by determining the exponent α_l and then using the generalized hyperscaling law along with our previous estimate of ν_{\perp} . As above remarked, the determination of the exponent α_l from our series is not yet accurate enough to be useful. It does suggest, however, that $\alpha_l = -0.02(2)$, which is compatible with the ϵ -expansion estimate in Table I. If, quite conservatively, we simply assume that α_l is negative and $|\alpha_l| < 0.1$, we get from the hyperscaling law the rough bounds $0.36 < \nu_{\parallel} < 0.52$, which are consistent with the $O(\epsilon^2)$ value $\nu_{\parallel} \approx 0.372$ reported in Table I. On the other hand, using the above reported estimate $\phi = 1.00(4)$ and the estimate $\beta_q = 0.40(2)$ given below, we get the value $\nu_{\parallel} = 0.40(3)$. Plugging back this result into the hyperscaling law, we find the value $\alpha_l = -0.01(6)$ for the specific-heat exponent, which is also compatible with all above indicated estimates. The values of the remaining exponents can all be obtained from the scaling laws.

We can thus conclude that our HT determinations of the critical exponents at the LP are in most cases consistent, to within $\approx 10\%$, with the ϵ -expansion estimates. In order to map out the branch of the critical line with $R < R_{LP}$, we have to analyze the wave-vector-dependent susceptibility $\chi(q_z, K_1, R)$. For $R < R_{LP}$ the critical point $K_{1c}(R)$ can be determined by locating the nearest positive singularity in K_1 of $\chi(q_z, K_1, R)$, with q_z near the peak value $\bar{q}_z = \bar{q}_z(K_1, R)$. The value of $K_{1c}(R)$ is taken to be the minimum with respect to q_z of the singularity locus $K_1 = K_1(q_z, R)$ of $\chi(q_z, K_1, R)$. Our results for the P - M branch of the critical line, also drawn in Fig. 1, complete the map of the boundary of the paramagnetic phase. In the same figure, we have schematically indicated a transition line, which separates the ferromagnetic and the modulated phases and joins the LP to the point $R = -1/4, T = 0$, where the ordering of the ground-state changes from ferromagnetic to modulated. This line is also expected to be of second order but is beyond the reach of our HT analysis. Our phase diagram agrees well with the cited results⁴⁶ obtained supplementing a MC simulation with the sixth-order HT expansions in Ref. 25.

It must be noted that the uncertainties of the points of the P - M branch of the critical line are sizably larger than those of the P - F branch, making it more difficult to obtain precise temperature-biased estimates of the critical exponents. If, nevertheless, we insist in computing some rough estimate of the exponent $\gamma(R)$, it is encouraging to observe that the results obtained from temperature-biased DAs remain essentially consistent, over a wide range of values of R , with those computed by the critical-point renormalization method which is insensitive to the uncertainties of the critical temperatures. The results for $\gamma(R)$ obtained by these two methods are reported in Fig. 9. For $R < -0.8$, on the left of the region of crossover from the value of γ_l , we observe that both sequences of estimates tend to stabilize at some value which is intermediate between those of the $O(2)$ and of the $O(3)$ universality classes. These puzzling results might deserve further confirmation by a MC study. If they are confirmed, the MC approach⁶⁷ would also be best suited to investigate whether a possible (weak) first-order⁶⁸ (rather than second-order) character of the P - M transition might explain its features. This possibility was suggested by a renormalization-group study of a Landau-Ginzburg effective four-component model of a biaxial $N=2$ system⁵³ which turned out to have only unstable fixed points at second order in the ϵ expansion.

The curve describing the peak value \bar{q}_z of the modulation wave number q_z at $T = T_c(R)$ vs R , obtained from our analysis, is reported in Fig. 10 and compared with the mean-field prediction $\bar{q}_z^{MF}(R) = \cos^{-1}(R_{LP}^{MF}/R)$, with $R_{LP}^{MF} = -1/4$. As pointed out in Ref. 25, also in the Ising case, at high temperature the peak of $\chi(q_z, K_1, R)$ occurs at $\bar{q}_z^{MF}(R)$ but, as the temperature decreases to $T_c(R)$, the peak moves to lower values of q_z for $R \gtrsim -0.6$ or otherwise to slightly higher values. This is clearly shown in Fig. 10. The largest deviations of our results from the mean-value approximation occur in a small vicinity of R_{LP} . From the behavior of this curve near $R \approx R_{LP}$, we have estimated the value $\beta_q = 0.40(2)$ used above.

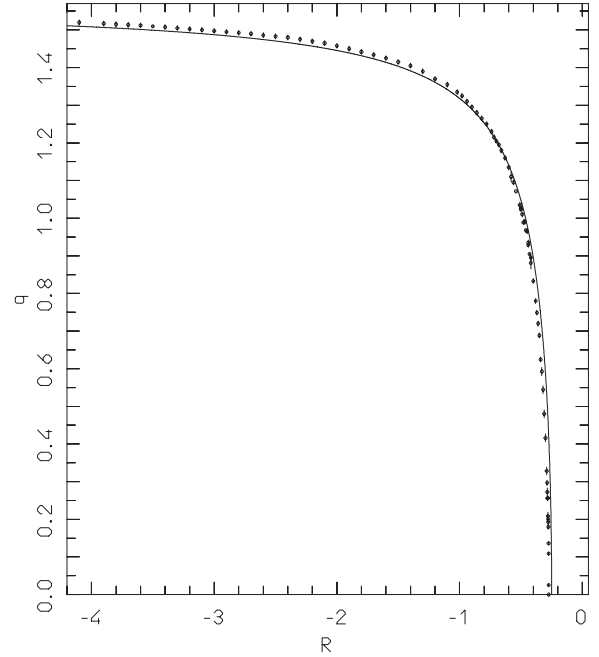


FIG. 10. The peak value of the modulation vector \bar{q}_z at the critical temperature plotted vs R for $R \leq R_{LP}$. The continuous curve represents the mean-field prediction $\bar{q}_z^{MF} = \cos^{-1}(R_{LP}^{MF}/R)$, with $R_{LP}^{MF} = -1/4$.

ACKNOWLEDGMENTS

This work was partially supported by the MIUR. We also thank the Physics Departments of Milano-Bicocca University and of Milano University for their hospitality and support. We are very grateful to W. Selke for critically reading the first draft of this paper and for calling our attention to some references. Our computations have been mostly performed by the *Turing* personal computer cluster of the Milano-Bicocca INFN Section. We also thank L. N. Shchur for granting us access to the *PARMA* cluster of the Landau Institute in Chernogolovka and Maria Medvedeva for her assistance.

APPENDIX: DERIVATION AND VALIDATION OF THE SERIES

We have used the algorithm⁶⁹ of the Schwinger-Dyson equations (SDEs) to compute the HT expansions for the N -vector spin models under study. When it was introduced, the SDE method could be profitably applied only to systems with nn interactions,⁷⁰ due to the severe limitations in the memory and speed of the computers available two decades ago. This method was repeatedly described in Refs. 70 and 71, and therefore it is sufficient to recall only that for the XY models described by the Hamiltonians (1) and (2), the SDEs take a particularly simple and suggestive form. Indicating by $\mathbf{s} = (\vec{x}_1, q_1; \vec{x}_2, q_2; \dots; \vec{x}_k, q_k)$ a set of site coordinates \vec{x}_i and of integer nonzero quantities q_i attached to them and such that $\sum_{i=1}^k q_i = 0$, the generic correlation function can be written as

$$\langle \phi(\mathbf{s}) \rangle = \frac{1}{Z} \int \Pi_x d\theta_x \phi(\mathbf{s}) e^{-\beta H}, \quad (\text{A1})$$

where $\phi(\mathbf{s}) = \exp[i \sum_k q_k \theta_{x_k}]$ and θ_x is the angle formed by the unit vector $\vec{v}(\vec{x})$ with a fixed direction. The SDE is

$$\begin{aligned} \langle \phi(\mathbf{s}) \rangle = & -\frac{K_1}{q_1} \sum_{\mu} (\langle \phi(\mathbf{s}_{\mu}^+) \rangle - \langle \phi(\mathbf{s}_{\mu}^-) \rangle) \\ & -\frac{K_2}{q_1} \sum_{\nu} (\langle \phi(\mathbf{s}_{\nu}^+) \rangle - \langle \phi(\mathbf{s}_{\nu}^-) \rangle). \end{aligned} \quad (\text{A2})$$

Here

$$\phi(\mathbf{s}_{\mu}^+) = \exp(i\theta_{x_1}) \exp(-i\theta_{x_1+a_{\mu}}) \phi(\mathbf{s}), \quad (\text{A3})$$

while

$$\phi(\mathbf{s}_{\mu}^-) = \exp(-i\theta_{x_1}) \exp(i\theta_{x_1+a_{\mu}}) \phi(\mathbf{s}). \quad (\text{A4})$$

Moreover

$$\phi(\mathbf{s}_{\nu}^+) = \exp(i\theta_{x_1}) \exp(-i\theta_{x_1+b_{\nu}}) \phi(\mathbf{s}), \quad (\text{A5})$$

and

$$\phi(\mathbf{s}_{\nu}^-) = \exp(-i\theta_{x_1}) \exp(i\theta_{x_1+b_{\nu}}) \phi(\mathbf{s}), \quad (\text{A6})$$

with \vec{x}_1 as an arbitrary site in the set \mathbf{s} . In the first sum of Eq. (A2), a_{μ} is the lattice vector joining the site \vec{x}_1 to the nn sites, whereas in the second sum b_{ν} denotes the vector joining the site \vec{x}_1 to the nnn sites in the case of the Hamiltonian [Eq. (1)] (the vector joining the site \vec{x}_1 to the sn sites in the case of the Hamiltonian [Eq. (2)]).

The computational complexity of the SDE method increases with the lattice dimensionality and, for a given dimensionality, with the effective coordination number, i.e., as the number of interacting neighbors increases. Essentially the same difficulty is met with the evaluation of the embedding factors in the conventional graph approach, but our method has the advantage of using the SDE as recurrence relations among the correlation functions and of requiring only a straightforward iteration of these relations, which avoids altogether all combinatorial intricacies of the graph method. In the specific cases under study, due to the presence of the nnn interactions, this method is, by some orders of magnitude, more memory and CPU demanding than for the pure nn interactions but otherwise not much more difficult. Thus, for example, in the computationally most intensive case, that of the Hamiltonian of Eq. (1) in $3d$ with *triaxial* interaction, the general SDE is a linear relationship among 25 *a priori* different correlation functions, while in the simpler nn interaction case in three dimensions, the SDE involves only 13 correlation functions.

A carefully designed code for the Schwinger-Dyson equations can compute moderately long series using only a reasonable CPU time of an ordinary 32-bit single-core processor desktop personal computer (PC). In particular, our codes can reproduce all previously existing series data in a negligible CPU time of the order of 10^{-3} s. Due to the sensitive dependence of the computational load on the effective coordination number, the series that we could derive for the uniaxial models are longer (and more fastly computed) than those for the d -axial models. In the case of the uniaxial model studied here, the expansion through order 17 was completed in approximately three weeks by a PC, while the order 18 was obtained by using a few nodes of a PC cluster for an equivalent single-processor CPU time of approximately five months. Longer series might be obtained by a more extensive parallelization of our codes or, perhaps, by returning to the conventional graph methods, provided that the efficiency of the current graph-embedding algorithms can be drastically improved.

The comparison of the extended expansions with independent, sufficiently long and reliable previous results is always a necessary step in the validation of the codes and of the results for automated derivations. Generally, in our case, this was not satisfactorily feasible. In two dimensions, a comparison was possible only for the uniaxial model [Eq. (1)], for which a fifth-order expansion of the susceptibility was tabulated in Ref. 40 and in three dimensions, only in the case of the uniaxial model, for which an expansion of the susceptibility was tabulated through sixth order in Ref. 25. Our series agree with these results. Due to the lack of other published data and to the present unavailability of old short unpublished series⁷² for the triaxial case in three dimensions, no further comparison with independent calculations was possible. Weaker (and obvious) tests, through all orders that we have computed, are feasible in the limiting cases⁷³ in which one of the exchange interaction constants vanishes. For example, when $K_2=0$, the series for the m -axial models should reduce to those of the nn interaction models on the same lattice. Therefore the series for the uniaxial models should reduce to those of a nn interaction model on the same lattice when $K_2=0$ and to those of a nn model on a $1d$ lattice when $K_1=0$. Of course, our results pass also these tests, which however pin down only two out of the $l+1$ coefficients of each order l . Our confidence in the correctness of the calculations, for which we have written two sets of largely independent codes, in Fortran and in C++ receives further support also from the stability of the numerical results under our many rewritings of both sets of codes to increase their efficiency, as well as from the smooth and consistent behavior of the quantities analyzed.

*paolo.butera@mib.infn.it

†mario.pernici@mi.infn.it

- ¹N. W. Dalton and D. W. Wood, *J. Math. Phys.* **10**, 1271 (1969); G. Paul and H. E. Stanley, *Phys. Lett.* **37A**, 328 (1971); G. Paul and H. E. Stanley, *Phys. Rev. B* **5**, 3715 (1972).
- ²J. Philhours, *Phys. Rev. B* **4**, 929 (1971).
- ³E. Luijten and H. W. J. Blöte, *Int. J. Mod. Phys. C* **6**, 359 (1995).
- ⁴A. Yoshimori, *J. Phys. Soc. Jpn.* **14**, 807 (1959); T. Kaplan, *Phys. Rev.* **116**, 888 (1959); J. Villain, *J. Phys. Chem. Solids* **11**, 303 (1959).
- ⁵R. J. Elliott, *Phys. Rev.* **124**, 346 (1961).
- ⁶W. Selke and M. E. Fisher, *Z. Phys. B: Condens. Matter* **40**, 71 (1980).
- ⁷J. Stephenson and D. D. Betts, *Phys. Rev. B* **2**, 2702 (1970); J. Stephenson, *Can. J. Phys.* **48**, 1724 (1970); J. Stephenson, *Phys. Rev. B* **1**, 4405 (1970); J. Stephenson, *ibid.* **15**, 5442 (1977); J. Stephenson, *ibid.* **15**, 5453 (1977).
- ⁸R. M. Hornreich, M. Luban, and S. Shtrikmann, *Phys. Rev. Lett.* **35**, 1678 (1975); M. Droz and M. D. Coutinho-Filho, *Proceedings of the 21st Conference on Magnetism and Magnetic Materials*, Philadelphia (AIP, New York, 1975); L. Kalok and G. M. Obermair, *J. Phys. C* **9**, 819 (1976).
- ⁹R. M. Hornreich, *J. Magn. Magn. Mater.* **15–18**, 387 (1980).
- ¹⁰M. E. Fisher, *Physica A* **106**, 28 (1981).
- ¹¹R. Liebmann, *Statistical Mechanics of Periodic Frustrated Systems*, Lecture Notes in Physics Vol. 251 (Springer, Berlin, 1986).
- ¹²W. Selke, *Phys. Rep.* **170**, 213 (1988).
- ¹³W. Selke, in *Phase Transitions and Critical Phenomena*, edited by C. Domb and J. Lebowitz (Academic, New York, 1992), Vol. 15.
- ¹⁴J. M. Yeomans, *Solid State Physics* (Academic, New York, 1988), Vo. 41, p. 151.
- ¹⁵M. Seul and D. Andelman, *Science* **267**, 476 (1995).
- ¹⁶H. T. Diep and H. Giacomini, in *Frustrated Spin Systems*, edited by H. T. Diep (World Scientific, Singapore, 2005).
- ¹⁷D. Loison, in *Frustrated Spin Systems*, edited by H. T. Diep (World Scientific, Singapore, 2005).
- ¹⁸H. W. Diehl, *Acta Phys. Slov.* **52**, 271 (2002); *Pramana* **64**, 803 (2005).
- ¹⁹A. Malakis, P. Kalozoumis, and N. Tyraskis, *Eur. Phys. J. B* **50**, 63 (2006).
- ²⁰G. Y. Chitov and C. Gros, *Low Temp. Phys.* **31**, 722 (2005).
- ²¹B. Widom, *J. Chem. Phys.* **84**, 6943 (1986).
- ²²Y. M. Vysochanskii and V. U. Slivka, *Usp. Fiz. Nauk* **162**, 139 (1992) [*Sov. Phys. Usp.* **35**, 123 (1992)]; F. S. Bates, W. Maurer, T. P. Lodge, M. F. Schulz, M. W. Matsen, K. Almdal, and K. Mortensen, *Phys. Rev. Lett.* **75**, 4429 (1995); D. Schwahn, K. Mortensen, H. Frielinghaus, and K. Almdal, *ibid.* **82**, 5056 (1999); M. Skarabot, R. Blinc, I. Musevic, A. Rastegar, and T. Rasing, *Phys. Rev. E* **61**, 3961 (2000); I. Luk'yanchuk, A. Jorio, and P. Saint-Gregoire, *Phys. Rev. B* **61**, 3147 (2000); C. C. Becerra, V. Bindilatti, and N. F. Oliveira, *ibid.* **62**, 8965 (2000); H. Weitzel, H. Ehrenberg, C. Heid, H. Fuess, and P. Burlet, *ibid.* **62**, 12146 (2000).
- ²³K. Symanzik, *Nucl. Phys. B* **226**, 187 (1983); B. Berg, S. Meyer, and I. Montvay, *ibid.* **235**, 149 (1984); M. Lüscher and P. Weisz, *Commun. Math. Phys.* **97**, 59 (1985).
- ²⁴B. Sheikholeslami and R. Wohlert, *Nucl. Phys. B* **259**, 572 (1985).
- ²⁵S. Redner and H. E. Stanley, *Phys. Rev. B* **16**, 4901 (1977); *J. Phys. C* **10**, 4765 (1977).
- ²⁶P. Butera and M. Comi, *Phys. Rev. B* **65**, 144431 (2002); P. Butera and M. Comi, *ibid.* **72**, 014442 (2005); *J. Stat. Phys.* **109**, 311 (2002).
- ²⁷P. Butera and M. Pernici, *Phys. Rev. B* **76**, 092406 (2007); arXiv:0806.1496, *Physica A* (to be published).
- ²⁸A. J. Guttmann, in *Phase Transitions and Critical Phenomena*, edited by C. Domb and J. Lebowitz (Academic, New York, 1989), Vol. 13.
- ²⁹M. Plischke and J. Oitmaa, *Phys. Rev. B* **19**, 487 (1979); J. Oitmaa, *J. Phys. A* **14**, 1159 (1981); J. Oitmaa, *ibid.* **18**, 365 (1985).
- ³⁰M. J. Velgakis and M. Ferer, *Phys. Rev. B* **27**, 401 (1983).
- ³¹J. Oitmaa and M. J. Velgakis, *J. Phys. A* **20**, 1495 (1987).
- ³²Z. Mo and M. Ferer, *Phys. Rev. B* **43**, 10890 (1991).
- ³³M. E. Fisher, in *Statistical Mechanics and Statistical Methods in Theory and Applications*, edited by U. Landman (Plenum, New York, 1977); M. E. Fisher and R. M. Kerr, *Phys. Rev. Lett.* **39**, 667(1977).
- ³⁴C. Alabiso and P. Butera, *J. Math. Phys.* **16**, 840 (1975).
- ³⁵J. Zinn-Justin, *J. Phys. (France)* **42**, 783 (1981).
- ³⁶J. H. Chen, M. E. Fisher, and B. G. Nickel, *Phys. Rev. Lett.* **48**, 630 (1982); M. E. Fisher and J. H. Chen, *J. Phys. (France)* **46**, 1645 (1985).
- ³⁷H. W. J. Blöte, E. Luijten, and J. Heringa, *J. Phys. A* **28**, 6289 (1995).
- ³⁸M. Campostrini, M. Hasenbusch, A. Pelissetto, P. Rossi, and E. Vicari, *Phys. Rev. B* **63**, 214503 (2001).
- ³⁹A. Soehanie and J. Oitmaa, *Mod. Phys. Lett. B* **11**, 609 (1997).
- ⁴⁰A. Clarizia, G. Cristofano, R. Musto, F. Nicodemi, and R. Pettorino, *Phys. Lett.* **148B**, 323 (1984).
- ⁴¹D. P. Landau, *J. Appl. Phys.* **42**, 1284 (1971); D. P. Landau, *Phys. Rev. B* **21**, 1285 (1980); D. P. Landau and K. Binder, *ibid.* **31**, 5946 (1985).
- ⁴²W. Selke, *Z. Phys. B* **29**, 133 (1978).
- ⁴³W. Selke and M. E. Fisher, *Phys. Rev. B* **20**, 257 (1979).
- ⁴⁴K. Kaski and W. Selke, *Phys. Rev. B* **31**, 3128 (1985).
- ⁴⁵M. Pleimling and M. Henkel, *Phys. Rev. Lett.* **87**, 125702 (2001).
- ⁴⁶W. Selke, *Solid State Commun.* **27**, 1417 (1978).
- ⁴⁷W. Selke, *J. Phys. C* **13**, L261 (1980).
- ⁴⁸J. F. Fernandez, M. Puma, and R. F. Angulo, *Phys. Rev. B* **44**, 10057 (1991).
- ⁴⁹D. Loison and P. Simon, *Phys. Rev. B* **61**, 6114 (2000).
- ⁵⁰H. W. Diehl and M. Shpot, *Phys. Rev. B* **62**, 12338 (2000); M. Shpot and H. W. Diehl, *Nucl. Phys. B* **612**, 340 (2001).
- ⁵¹M. M. Leite, *Phys. Rev. B* **67**, 104415 (2003); C. Mergulhão, Jr. and C. E. I. Carneiro, *ibid.* **58**, 6047 (1998); C. Mergulhão, Jr. and C. E. I. Carneiro, *ibid.* **59**, 13954 (1999); P. R. S. Carvalho and M. M. Leite, arXiv:0704.3208 (unpublished).
- ⁵²C. Bervillier, *Phys. Lett. A* **331**, 110 (2004).
- ⁵³T. Garel and P. Pfeuty, *J. Phys. C* **9**, L245 (1976).
- ⁵⁴A. Aharony and D. Mukamel, *J. Phys. C* **13**, L255 (1980).
- ⁵⁵M. A. Shpot, Yu. M. Pis'mak, and H. W. Diehl, *J. Phys.: Condens. Matter* **17**, S1947 (2005).
- ⁵⁶R. M. Hornreich, M. Luban, and S. Shtrikmann, *Phys. Lett.* **55A**, 269 (1975).
- ⁵⁷D. Mukamel, *J. Phys. A* **10**, 1249 (1977); R. M. Hornreich and A. D. Bruce, *ibid.* **11**, 595 (1978).
- ⁵⁸P. Butera and M. Comi, *Phys. Rev. B* **56**, 8212 (1997).

- ⁵⁹A. J. Liu and M. E. Fisher, J. Stat. Phys. **58**, 431 (1990).
- ⁶⁰D. L. Hunter and G. A. Baker, Phys. Rev. B **7**, 3346 (1973).
- ⁶¹P. Butera and M. Comi, Phys. Rev. B **60**, 6749 (1999).
- ⁶²M. Hasenbusch and T. Török, J. Phys. A **32**, 6361 (1999).
- ⁶³E. Burovski, J. Machta, N. Prokof'ev, and B. Svistunov, Phys. Rev. B **74**, 132502 (2006).
- ⁶⁴K. S. D. Beach, arXiv:cond-mat/0507541 (unpublished).
- ⁶⁵J. A. Lipa, J. A. Nissen, D. A. Stricker, D. R. Swanson, and T. C. P. Chui, Phys. Rev. B **68**, 174518 (2003).
- ⁶⁶I. Nasser and R. Folk, Phys. Rev. B **52**, 15799 (1995).
- ⁶⁷V. Thanh Ngo and H. T. Diep, J. Appl. Phys. **103**, 07C712 (2008).
- ⁶⁸M. Tissier, B. Delamotte, and D. Mouhanna, Phys. Rev. B **67**, 134422 (2003).
- ⁶⁹P. Butera, M. Comi, and G. Marchesini, Phys. Rev. B **33**, 4725 (1986).
- ⁷⁰P. Butera, M. Comi, and G. Marchesini, Nucl. Phys. B **300**, 1 (1988); P. Butera, M. Comi, and G. Marchesini, Phys. Rev. B **40**, 534 (1989); P. Butera and M. Comi, *ibid.* **46**, 11141 (1992); P. Butera and M. Comi, *ibid.* **50**, 3052 (1994).
- ⁷¹P. Butera, R. Cabassi, M. Comi, and G. Marchesini, Comput. Phys. Commun. **44**, 143 (1987); P. Butera and M. Comi, Ann. Comb. **3**, 277 (1999).
- ⁷²S. Redner (private communication).
- ⁷³P. Butera and M. Comi, Phys. Rev. B **54**, 15828 (1996).